Available online at www.sciencedirect.com
SCIENCE DIRECT®
Atmospheric Environment 39 (2005) 1393–1404
ATMOSPHERIC ENVIRONMENT
www.elsevier.com/locate/atmosenv

# Hygroscopic growth behavior of a carbon-dominated aerosol in Yosemite National Park

Christian M. Carrico[a,*], Sonia M. Kreidenweis[a], William C. Malm[b], Derek E. Day[b], Taehyoung Lee[a], Jacqueline Carrillo[a], Gavin R. McMeeking[a], Jeffrey L. Collett Jr.[a]

[a]*Department of Atmospheric Science, Colorado State University, Ft. Collins, CO 80523, USA*
[b]*Cooperative Institute for Research of the Atmosphere/National Park Service, Colorado State University, Ft. Collins, CO 80523, USA*

Received 4 August 2004; received in revised form 15 November 2004; accepted 15 November 2004

**Abstract**

The influence of particulate organic material (POM) and the contribution of biomass smoke on air quality and visibility remain a paramount issue in addressing regional haze concerns in US national parks. Measurements during the Yosemite Aerosol Characterization Study (July–September 2002) indicated an aerosol dominated by POM (~70% of identified species) and strongly influenced by biomass smoke. Here we report aerosol size hygroscopic growth measurements for dry (RH < 5%) aerosol diameters of 100 and 200 nm as measured with a controlled relative humidity tandem differential mobility analyzer. Hygroscopic growth was found to be negligible for relative humidity (RH) < ~40% within the sensitivity of the method. For RH > 40%, particle size typically increased smoothly with RH, and overall hygroscopic growth at high RH was low to moderate in comparison to the range of values reported in the literature. For RH > 80%, both monomodal and bimodal growth profiles were observed during the study, with 200 nm particles more often splitting into bimodal profiles (68% of cases), indicating some degree of external mixing. Trimodal growth profiles were observed on two occasions during periods of changing meteorology and aerosol composition. For bimodal profiles for 200 nm dry particles, particle diameter growth factors at RH = 80% ($D(\mathrm{RH}=80\%)/D_o$ where $D_o$ is measured at RH < 5%) were $1.11 \pm 0.04$ and $1.29 \pm 0.08$ for the more and less hygroscopic modes, respectively. Ensemble $D/D_o$ was calculated using a cubic-weighted sum of $D/D_o$ of individual modes. For 200 nm particles, average ensemble $D(\mathrm{RH}=80\%)/D_o$ was $1.15 \pm 0.05$ and $D(\mathrm{RH}=90\%)/D_o$ was $1.31 \pm 0.06$, and were slightly large for 100 nm particles. These growth factors are dramatically lower than those for typical ambient aerosol ionic components such as sulfate, nitrate and sodium salts and sulfuric acid. An inverse relationship between the POM fraction of $PM_{2.5}$ and hygroscopicity was particularly evident for 200 nm particles with $D(\mathrm{RH}=80\%)/D_o$ approaching ~1.1 as the POM/ionic mass ratio exceeded 10. Linear correlations with several measurements of POM and select biomass smoke markers were $-0.74 < R < -0.59$ for 200 nm and $-0.43 < R < -0.25$ for 100 nm particles. The limited hygroscopic growth of the carbon dominated, biomass smoke influenced aerosol at Yosemite has important implications to assessing the role of POM in visibility degradation in national parks.


*Keywords:* $PM_{2.5}$; Regional haze; Organic carbon; Biomass smoke; Tandem differential mobility analyzer; Secondary organic aerosol

*Corresponding author. Tel.: +1 970 491 8667; fax: +1 970 491 8483.
*E-mail address:* carrico@lamar.colostate.edu (C.M. Carrico).

1352-2310/$ - see front matter © 2004 Elsevier Ltd. All rights reserved.
doi:10.1016/j.atmosenv.2004.11.029

## 1. Introduction

### 1.1. Carbonaceous aerosol, biomass burning, and air quality

Emissions from biomass burning are a major global source of particulate organic material (POM), and cause severe impacts on regional to continental scale air quality (Wotawa and Trainer, 2000; Kreidenweis et al., 2001). Pyrogenic aerosols are important to visibility degradation, affect aquatic ecosystems and terrestrial vegetation, and potentially have human health consequences (McKenzie et al., 1995; Riebau and Fox, 2001; Sullivan et al., 2001). Furthermore, smoke can have significant effects on the global radiation budget and climate (Penner et al., 1992; Hobbs et al., 1997). However, the contribution of smoke from prescribed burns and wildfires to regional haze in the US is poorly characterized. The US Environmental Protection Agency's (US EPA's) Regional Haze Rule requires Class I areas (national parks and pristine areas) to attain natural background visual air quality by the middle of this century (US EPA, 1999). Biogenic, pyrogenic and anthropogenic sources of POM, often difficult to separate, must be considered in air quality and forest management strategies to attain these goals.

Inland national parks of California such as Sequoia, Joshua Tree, and Yosemite are typically among the most air quality-impacted parks in the western US (Sullivan et al., 2001). IMPROVE network measurements show that fine mode particulate matter concentrations ($PM_{2.5}$) and visibility in western national parks are strongly impacted by POM (Malm et al., 2004). Models suggest that pyrogenic and biogenic sources dominate POM in this region, particularly in summer (Park et al., 2003). The Yosemite Aerosol Characterization Study (YACS, mid-July to early September 2002) sought to characterize aerosol chemical, physical, and optical properties and the relationships of these parameters to visibility. Measurements were made at Turtleback Dome on the south rim of Yosemite Valley (IMPROVE monitoring site at 119.70 W; Lat 37.71 N; Elevation 1615 m) and are described fully in Malm et al. (2005). Here we focus on measurements of aerosol water uptake completed during the study.

### 1.2. Hygroscopicity and particulate organic material

Modeling studies show atmospheric light extinction is critically dependent on aerosol phase water (Pilinis et al., 1995; Malm and Kreidenweis, 1997; Malm et al., 2003). Lab studies of water uptake by mixtures of POM with inorganic salts generally have found a lower deliquescence point and lower hygroscopicity for the mixtures than for pure salts such as NaCl and $(NH_4)_2SO_4$ (Hansson et al., 1998; Prenni et al., 2003; Brooks et al., 2004). Nonetheless, some organic species uptake water, though the precise hygroscopic behavior of ambient POM is poorly characterized and appears to vary with POM source and composition (Saxena and Hildemann, 1996). This is particularly relevant for biomass smoke aerosols, comprised of POM and often mixed with small contributions of inorganic constituents.

As particles grow with increasing RH, separation into "more" and "less" hygroscopic modes (and sometimes additional modes) is often observed, indicative of externally mixed particles (Zhang et al., 1993). A review of ambient hygroscopic growth measurements by Cocker et al. (2001) found a broad range of results for diameter growth factors as a function of RH ($D$(RH)/$D_o$, where $D_o$ is the particle diameter at a low reference RH "dry" conditions). Typically, though, there was a less hygroscopic mode with $D$(high RH)/$D_o$ of 1– 1.4 and a more hygroscopic mode in the range of 1.1–1.8 for high RH in the range of 80–90%, depending on the study. This same study, based in Pasadena, California, also found enhanced hygroscopic growth during periods influenced by nearby forest fires (Cocker et al., 2001). Aircraft measurements of smoke in South America have shown nearly hygrophobic aerosol in fresh smoke and modest enhancements in hygroscopicity as the smoke ages (Kotchenruther and Hobbs, 1998). Likewise, models have invoked diverse assumptions ranging from the suppression of inorganic water uptake by the presence of POM to POM hygroscopicity equaling that of $(NH_4)_2SO_4$ (Saxena et al., 1995; Iacobellis et al., 1999; Malm and Day, 2001; Markowicz et al., 2003). The hygroscopic behavior of POM and biomass smoke are uncertain though key determinants of visibility impacts in scenic areas and potential climate influences.

## 2. Experimental methods

The results presented here are derived from measurements from a hygroscopic tandem differential mobility analyzer (HTDMA) (Rader and McMurry, 1986). The instrument includes two electrostatic classifiers plumbed in series (DMA, TSI Inc. Model 3071), each interfaced to a condensation particle counter (CPC, TSI Inc. Model 3010-S). It is described below and in more detail in Brechtel and Kreidenweis (2000) and Prenni et al. (2003) (Fig. 1). Each ~5-h measurement cycle with the instrument (2 dry diameters and 7–8 RH set points) typically occurred during the daytime hours after winds shifted to upslope (10:00–18:00 US Pacific Standard Time). Custom software (National Instruments, Inc. Labview) was used for instrument control and data acquisition. Ambient air was sampled through a rooftop inlet, exited a desiccant drier at RH = 11% ± 2%, and is reduced to RH = 1.7% ± 0.3% by the exit of DMA1 (Fig. 1).

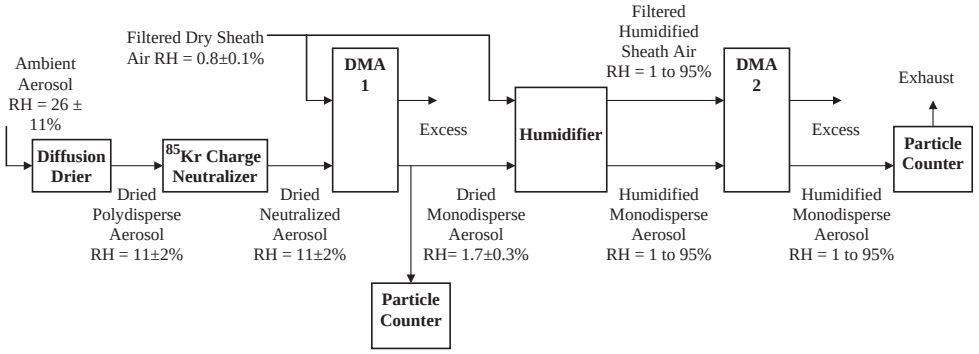


Fig. 1. Flow diagram of the hygroscopic tandem differential mobility analyzer (HTDMA).

The dry monodisperse aerosol exiting DMA1 was split between a CPC and a humidification system. The humidifier used a water vapor permeable Nafion membrane with an RH controlled purge flow (MD-110-48SS, Permapure, Inc.). The aerosol sample residence time downstream of the humidifier before entering DMA2 was approx. 2.5 sec. The humidity controlled purge flow was subsequently used as the sheath flow for the second, humidified DMA2 to assure constant RH through DMA2. Particle losses in the plumbing were corrected for and ranged from 9% for the largest size measured here (340 nm) to 13% for the smallest size measured here (100 nm). Both DMAs were operated at sheath to sample flow ratios of 10–1.

Growth factors at a specified RH, $D(\mathrm{RH})/D_o$ (where $D_o$ is the "dry" diameter measured at RH $<5\%$ here), were determined using the TDMAFIT program (Zhou et al., 2002) as described by Stolzenburg and McMurry (1988). In cases with multiple modes, an ensemble $D/D_o$ was calculated from the $D/D_o$ for individual modes according to $(D/D_o)^3_{ens} = x_1(D/D_o)^3_1 + (1-x_1)(D/D_o)^3_2$, where the subscripts refer to the mode and $x_1$ is the number fraction in mode 1. This ensemble was used to specify qualitatively whether the "more" or "less" hygroscopic mode dominated in bimodal profiles. A step change in $D/D_o$ between RH = 70% and 80% set points was interpreted as qualitative evidence of deliquescence of one or more aerosol components.

## 3. Results and discussion

### 3.1. Quality control

Previous investigators have found uncertainties in particle sizing using DMAs of 1–5% of the measured diameter (McMurry and Stoltzenburg, 1989; Zhang et al., 1993; Brechtel and Kreidenweis, 2000; Brooks et al., 2004). One measure of the uncertainty derives from the DMA2 measured growth factor of the quasi-monodispersion exiting DMA1. The growth factor measured without sample conditioning between DMA1 and DMA2 with ambient aerosol was $D_{DMA2}/D_{DMA1}$ (RH $<5\%$) $= 0.997 \pm 0.006$ ($n = 91$ removing one outlier) and ranged from 0.986 to 1.014. Similarly, based on propagated uncertainties in the flow rate, voltage, temperature and pressure, the overall uncertainty in $D/D_o$ is taken here as $\pm 0.02$ in absolute units. Flows were checked (Sensidyne Inc. Gilibrator) and adjusted before each experiment with a coefficient of variation (standard deviation divided by mean) of 0.012 for the smallest flow (0.5 lpm) and less for the larger flows (1, 5, 15 lpm).

RH uncertainty is calculated from the difference between collocated measurements of the RH on the sheath and polydisperse flows of DMA2. A regression plot of RH sheath vs. RH sample of DMA2 gives a slope of 0.98, and offset of 0.5% and $R^2$ of 0.998. The average magnitude of the difference in RH measurements for the sample and sheath flows in DMA2 (i.e. absolute value of sample2-sheath2) was $1.18 \pm 0.61$ in % RH units for $n = 375$ samples (removing 7 outliers). Taking the mean $\pm$ two standard deviations gives an uncertainty of $\pm 2.4\%$ in % RH units. An average of the two sensors will yield a lower uncertainty, and the overall uncertainty in RH measurement adopted for these results is $\pm 2\%$. This is similar to the manufacturer's rated accuracy of $\pm 1.5\%$.

RH and temperature were measured at several locations within the instrument with six recently manufacturer-calibrated capacitive-type RH sensors (Rotronic, Inc. Model Hygroclip S). The entire apparatus was in a temperature-controlled enclosure that was constantly mixed with fans to keep the system as isothermal as possible. Most of the temperature variability was due to diurnal and instrumentation heating that the trailer climate control could not overcome. The measurements occurred at average $T = 31.6 \pm 2.0\,^{\circ}\mathrm{C}$. Based on 12 sensors, the difference between the maximum and minimum temperature point in the entire system was $1.3 \pm 0.7\,^{\circ}\mathrm{C}$. Temperature

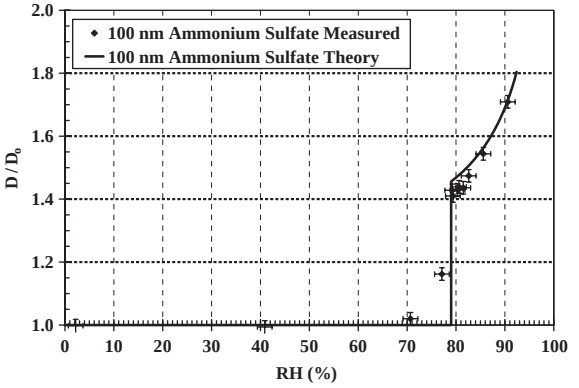


Fig. 2. Comparison of field measured and predicted values for $D/D_o$ (RH) for 100 nm dry diameter ammonium sulfate particles. Error bars represent uncertainty of $\pm 0.02$ for $D/D_o$ and $\pm 2\%$ in RH.

uniformity assures a minimization of unintended RH gradients through the sample flow. Based on temperature measurements at the inlet and outlet of DMA2, the absolute value of the difference in inlet and outlet temperatures was $0.12 + 0.11\,^{\circ}C$ ($n = 205$ samples, removing 7 outliers) which corresponds to an RH gradient through DMA2 of ~0.6% at RH = 90%.

System performance was tested during YACS by measuring the hygroscopic growth of aerosol with known hygroscopic properties. Measurement of laboratory generated test aerosol was completed on 29 August 2002, approximately 1 week before the end of the experiment. Test aerosol was generated with an atomizer (TSI, Inc., Model 9302A) using a pure $(NH_4)_2SO_4$ solution. Measurement with 100 nm pure $(NH_4)_2SO_4$ shows agreement with modeled growth factors within several percent using thermodynamic data from Tang and Munkelwitz (1994) (Fig. 2). Measured $D/D_o$ at RH = 80.2±0.9% ($n = 5$) and RH = 90.2% ($n = 1$) were 1.44±0.01 and 1.72, respectively, compared with theoretical values of 1.47 and 1.70, respectively, similar to the 0.02 estimated uncertainty. Measured deliquescence occurred over 77% < RH < 80% due to slight RH gradients within the humidifier, similar to Prenni et al. (2003) and in agreement with Tang and Munkelwitz (1993) who report 79% at $T = 30\,^{\circ}C$.

### 3.2. Ambient aerosol chemical composition and meteorological context

Prevailing meteorology was hot and dry during the entire study. Experiment average ($n = 1248$ hourly averages) temperature and relative humidity (RH) were 21.1±4.6 °C and 33±11% while daytime averages during which these measurements occurred were 25.0±3.4 °C and 26±9% ($n = 368$ hourly averages from 1000–1800 local), respectively. Aside from light precipitation on the first and the last days of YACS, conditions were dry. Generally, upslope westerly flow each morning initiated transport of hazy boundary-layer air from the valleys below, and winds calmed or changed to easterlies in the evening (Malm et al., 2005).

Summer 2002 featured poor air quality in central California and Yosemite and was an active fire season in the US west. (http://www.arb.ca.gov/homepage.htm) (Malm et al., 2005). Over one hundred thousand acres burned in Oregon and California during YACS, and a number of smaller local fires burned within the park (http://www.nifc.gov/fireinfo/2002/summary.html). Satellite imagery (MODIS; http://:visibleearth.nasa.gov) suggests smoke from these fires affected Yosemite. Chemical analyses of samples from YACS showed POM to be the dominant contributor to $PM_{2.5}$, ranging from 1 to ~20 $\mu g\,m^{-3}$ and on average representing ~70% of identified species (OC to POM multiplier of 1.8). The remaining $PM_{2.5}$ mass was primarily $SO_4^{2-}$ and $NH_4^+$ (Malm et al., 2005). Based on IMPROVE network data, average reconstructed $PM_{2.5}$ at Yosemite peaks during the summer (~8 $\mu g m^{-3}$ during JJA of 1996–1999) with >50% contribution from POM (OC to POM multiplier of 1.8) (Malm et al., 2005).

### 3.3. Measurements of ambient aerosol hygroscopic growth at yosemite during YACS

Typically, $D/D_o$ profiles as a function of RH showed measurable hygroscopic growth initiated at RH~40%. On average, the Yosemite aerosol followed a smooth growth profile (Fig. 3). Hygroscopic growth for RH > 80% was much smaller than that for pure ammonium sulfate (Fig. 3, Table 1). Clear evidence of deliquescence was apparent for a minority of the measurements, 33% and 24% of 100 and 200 nm profiles, respectively. When deliquescence was apparent, it typically occurred at RH = 80% and often featured a split into two modes of "more" and "less" hygroscopic populations. It should be reiterated that here the determination of deliquescence is strictly qualitative due to the limited RH resolution of the measurement. Composition measurements during YACS indicated that over 80% of the ionic composition of $PM_{2.5}$ at Yosemite consisted of sulfate, ammonium and nitrate, in order of importance (Malm et al., 2005). Polluted aerosols whose ionic composition is dominated by ammoniated sulfates typically demonstrate deliquescence in the range 70% < RH < 80% (Carrico et al., 2003), similar to the RH range where deliquescence, if any evidence was observed of it, during YACS.

Overall, observed hygroscopic properties of 100 and 200 nm particles show similar magnitude and structure on average amongst both modes 1 and 2 and the

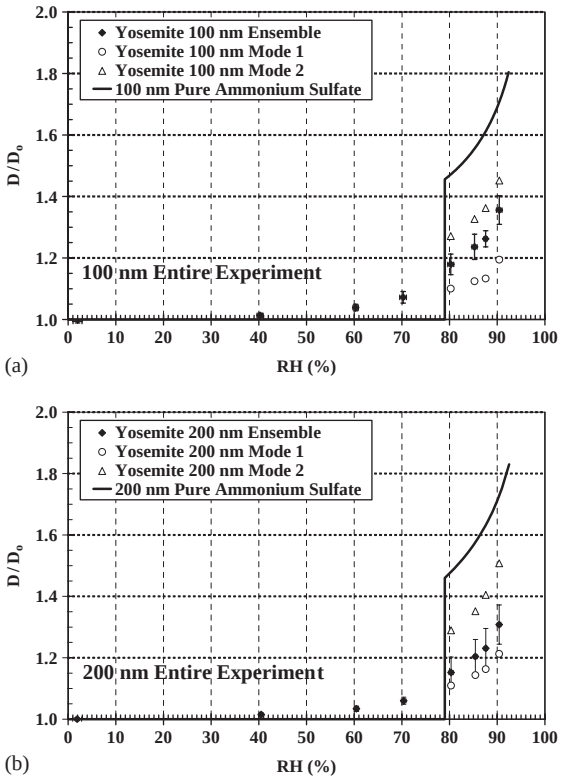


Fig. 3. Experiment average mean and standard deviation diameter growth factors ($D$ (RH)/$D_o$) vs. RH for (a) 100 nm particles and (b) 200 nm particles. A cubic weighted ensemble $D/D_o$ and for individual modes 1 and 2 when a bimodal growth profile occurred are shown. In comparison is the theoretical growth curve for pure $(NH_4)_2SO_4$. Standard deviations for $D/D_o$ and RH are shown.

ensemble (Fig. 3, Table 1). However, the prevalence of bimodal profiles was different comparing 100 and 200 nm particles (Table 2). For low RH $<80\%$, clear separation of "more" and "less" hygroscopic modes was not typically apparent. Emerging for RH $>80\%$, bimodal growth profiles were observed with 27% and 68% of the measurements for 100 and 200 nm particles, respectively. Among the bimodal cases for 200 nm particles, the less hygroscopic mode typically dominated the hygroscopic growth characteristics (84% of cases), based on the ensemble weighting described in the methods. The more hygroscopic mode of particles dominated 100 nm bimodal profiles (58% of the cases). This shows external mixing of the more and less hygroscopic components. Nevertheless, it should be noted that the less hygroscopic mode did grow, while the more hygroscopic mode was less typically less hygroscopic than $(NH_4)_2SO_4$ suggesting the more and less hygroscopic modes were not populations of single component chemically "pure" constituents confirmed from individual particle analysis (Hand et al., 2005).

Table 1
Summary of aerosol diameter growth factors ($D/D_o$) for dry diameters of 100 and 200 nm during the Yosemite Aerosol Characterization Study in summer 2002

| Dry $D$ (nm) | $N$ | $D$(RH = 40%)/$D_o$ | $D$(RH = 60%)/$D_o$ | $D$(RH = 70%)/$D_o$ | Ensemble $D$(RH = 80%)/$D_o$ | Less hygro mode $D$(RH = 80%)/$D_o$ | More hygro mode $D$(RH = 80%)/$D_o$ | Ensemble $D$(RH = 90%)/$D_o$ | Less hygro mode $D$(RH = 90%)/$D_o$ | More hygro mode $D$(RH = 90%)/$D_o$ |
|---|---|---|---|---|---|---|---|---|---|---|
| 100 | 45 | 1.01±0.01 | 1.04±0.01 | 1.07±0.02 | 1.18±0.03 | 1.10±0.08 | 1.27±0.11 | 1.36±0.05 | 1.19±0.11 | 1.45±0.12 |
| 200 | 47 | 1.01±0.01 | 1.03±0.01 | 1.06±0.01 | 1.15±0.05 | 1.11±0.04 | 1.29±0.08 | 1.31±0.06 | 1.21±0.07 | 1.51±0.10 |

For growth profiles that split into two growth modes at RH $>80\%$, $D/D_o$ are given for the less and more hygroscopic modes. As given in the methods, ensemble $D/D_o$ growth factors are found from a cubic weighting of $D/D_o$ for individual modes and are shown for RH $=80\%$ and 90%. In comparison, 100 nm particles of pure sulfuric acid and ammoniated sulfates have $1.5<D/D_o$ (RH $=80\%$) $<1.8$ and $1.7<D/D_o$ (RH $=90\%$) $<2.2$ and pure NaCl grows by factors of 2 and 2.5, respectively.

Table 2
Summary of aerosol hygroscopic properties during the Yosemite Aerosol Characterization Study in summer 2002

| Dry $D$ (nm) | $N$ | Monomodal | Bimodal | Dominant mode | Deliquescence evidence |
|---|---|---|---|---|---|
| 100 | 45 | 33 (73% of cases) | 12 (27%) | 7-More hygroscopic (58%) | 15 (33%) |
| 200 | 47 | 15 (32% of cases) | 32 (68%) | 27-Less hygroscopic (84%) | 11 (24%) |

The number and percentage of measurements in each category (monomodal vs. bimodal, the dominant mode for bimodal profiles) is also given.

Based on the Kelvin effect alone, 100 nm particles would be expected to have slightly lower $D/D_o$ (e.g., 1.69 vs. 1.71 at RH = 90% for pure $(NH_4)_2SO_4$). On average, growth factor values did not differ significantly comparing 100 and 200 nm particles (Fig. 3). For 200 nm particles, average $D(RH = 80\%)/D_o$ values for the less and more hygroscopic modes were $1.11 \pm 0.04$ and $1.29 \pm 0.08$, respectively, and similar for 100 nm particles (Table 1). $D/D_o$ at low RH and for respective modes at high RH comparing 100 and 200 nm particles were not different at any confidence level above 90% based on the $t$ statistic (0.4 and 0.3 for less and more hygroscopic modes, respectively). However, average ensemble $D(RH = 80\%)/D_o$ were 1.15 and 1.18 for 200 and 100 nm particles, respectively, and the $t$ statistic (3.0) shows they were different from >99% confidence. This is attributed to the relative number of particles in the more or less hygroscopic modes rather than sharply contrasting composition differences between 100 and 200 nm particles.

Trimodal profiles of $D/D_o$ were observed on 18 August and 2 September 2002 (DOY 230 and 245) when a shift was occurring from overnight stagnant or downslope flow to daytime upslope westerlies (Fig. 4). Likely a result of mixing of distinct air masses, growth profiles for 100 and 200 nm particles on 2 September featured modes with $D(RH = 90\%)/D_o = 1.6, 1.3$, and 1.05. These three $D/D_o$ values are similar to that of pure $(NH_4)_2SO_4$, the experiment-average ensemble $D/D_o$ during YACS, and that of a nearly hygrophobic mode, respectively (Fig. 4a, b). Though the data were somewhat noisy due to the low counting statistics during this relatively clean period, the trimodal profile was present for all measurements with RH > 80% and for both dry sizes. Likewise on 18 August 2002 when similar meteorological changes were occurring, a trimodal distribution with similar modes was seen for 100 nm particles (Fig. 4c). The absence of a strongly hygroscopic mode for 200 nm particles is attributed to the dominance of aged smoke particles with low hygroscopicity in this size range as is discussed in greater depth in the next section.

Average ambient RH during the study was low ($33 \pm 11\%$ overall and $26 \pm 9\%$ during daytime), with RH exceeding 70% only twice (both at night). Thus, ambient aerosol water content was likely quite small, and the average expected $D(RH = \text{ambient})/D_o$ is

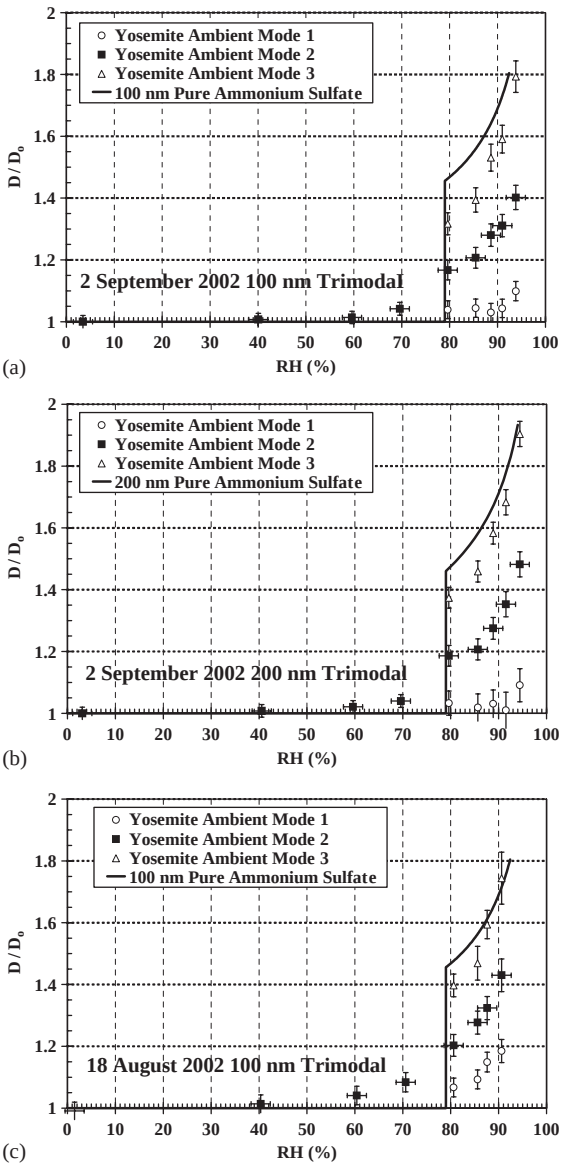


Fig. 4. Diameter growth factors ($D/D_o$ (RH)) vs. RH on 2 September (DOY 245) when a trimodal growth profile was observed for (a) 100 nm dry particles and (b) 200 nm dry particles, and (c) on 18 August (DOY 230) when a trimodal growth profile was observed for 100 nm particles. Uncertainties are shown as error bars.

estimated as below detection limits of the measurement (1.02), indicating a limited role of aerosol phase water in visibility degradation at Yosemite during summer. Two qualifications must be made to the above, though, regarding (1) the ambient hydration state of the particles and (2) the size range of particles most important to visibility impacts. Under the assumption that the measured $D/D_o$ were, as intended, on the lower deliquescent branch of the hysteresis loop, the existence of the ambient aerosol on the metastable branch of the hysteresis loop may result in larger ambient aerosol phase water. Conversely, even at the low RH experienced by the particles (RH < 5%) as they were dried before rehumidification, the particles may not have completely dried as has been found for some organic compounds and $NH_4NO_3$ in some experiments. Thus the "dry" diameters $D_o$ to which the $D/D_o$ growth factors were normalized may have retained some very small quantity of aerosol phase water. Secondly, the measurements presented here are for discrete sizes of 100 and 200 nm that represent only a subset of the entire population, and a direct extrapolation to the hygroscopic growth properties at other sizes or in the bulk aerosol is not possible.

### 3.4. Relationship of hygroscopicity to chemical composition and smoke influence

Observed hygroscopic growth, considerably lower than that observed with salts and acidic species

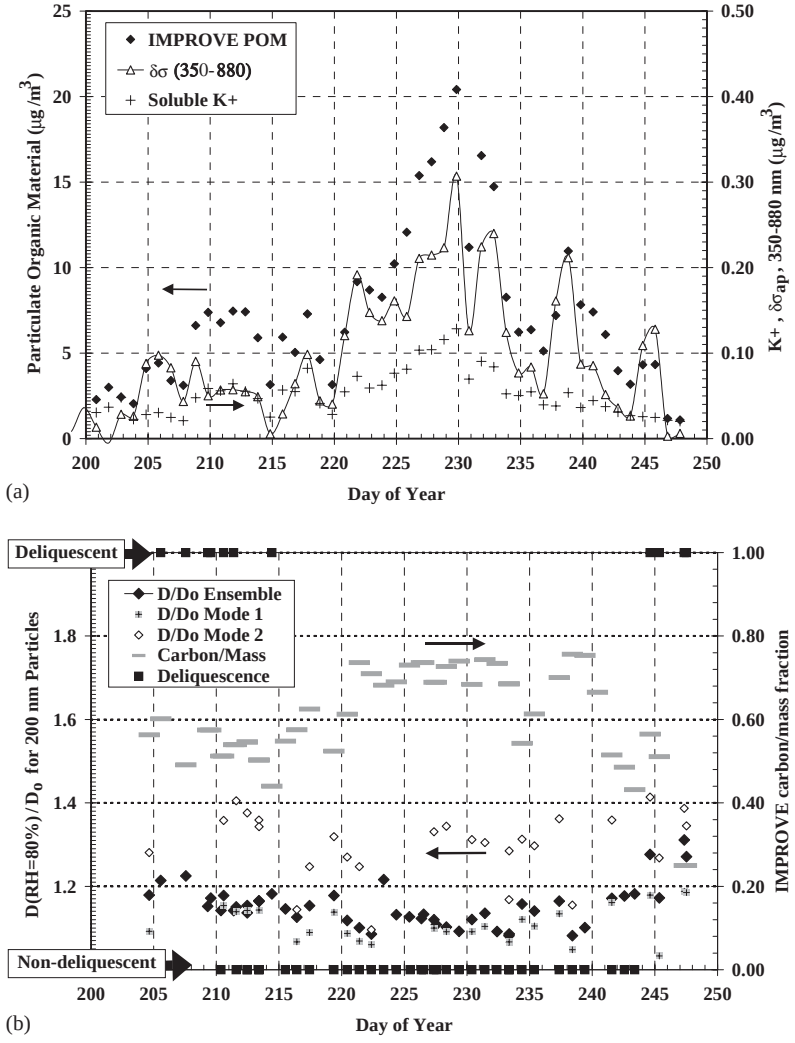


Fig. 5. Time series (a) of 24 h average POM (from 24 h IMPROVE sampler assuming a carbon to POM multiplier of 1.8), soluble potassium ($K^+$, 24 h URG filter samples), and the difference in UV and IR wavelength measurements of "black carbon" from an aethalometer (350–880 nm). Time series (b) of $D/D_o$ (80%) for 200 nm particles, $PM_{2.5}$ carbon/$PM_{2.5}$ mass (IMPROVE), and a qualitative indicator for the observation of deliquescent hygroscopic growth for 200 nm particles.

containing sulfate, nitrate and chloride, is now examined in relation to aerosol chemical composition. Time series of $D(\mathrm{RH}=80\%)/D_o$ for 200 nm dry particles are shown in Fig. 5 along with an indicator of aerosol chemical composition, the carbon mass fraction. $D/D_o$ is given independently for the less (Mode 1) and more (Mode 2) hygroscopic aerosol as well as an ensemble based on cubic weighted combination of modes as described in the methods. Also indicated qualitatively on the top and bottom margins of the time series is whether the aerosol hygroscopic growth showed strongly deliquescent features. Overall, the middle of August (DOY 225–230) featured the largest POM contribution. It also featured the lowest $D(\mathrm{RH}=80\%)/D_o$, and typically monotonic, rather than deliquescent growth. These measurements are consistent with laboratory experiments on mixtures of salts with organic species that show a lowering of hygroscopic growth and the smoothing of clear deliquescence points with increasing organic fraction (Hansson et al., 1998; Ansari and Pandis, 2000; Prenni et al., 2003).

Although on average the hygroscopic properties of 100 and 200 nm particles are quite similar, during select periods notable differences were observed. Changes in the dry size distribution during the middle of August indicated a shift to a bimodal number distribution featuring an accumulation mode with $D_{g,v}$~0.4 um and thought to be dominated by aged smoke (McMeeking et al., 2005; Malm et al., 2005). During this period, 100 and 200 nm particles resided in distinct modes of the dry size distribution (Fig. 6a), where 200 nm particles were a part of an accumulation mode arriving at Yosemite and associated with aged smoke (McMeeking et al., 2005). Hygroscopic growth of the 200 nm particles was observed to be considerably lower than that for 100 nm particles (Fig. 7a). In contrast, during the relatively "clean" period on 4 September 2002, both 100 nm and 200 nm particles showed similar hygroscopic growth properties, both with evidence of deliquescence and bimodality (Fig. 7b). Dry size distributions during such "clean" periods often featured a single mode encompassing 100 and 200 nm particles and at times the appearance of an ultrafine mode $D_p$~50 nm as shown in

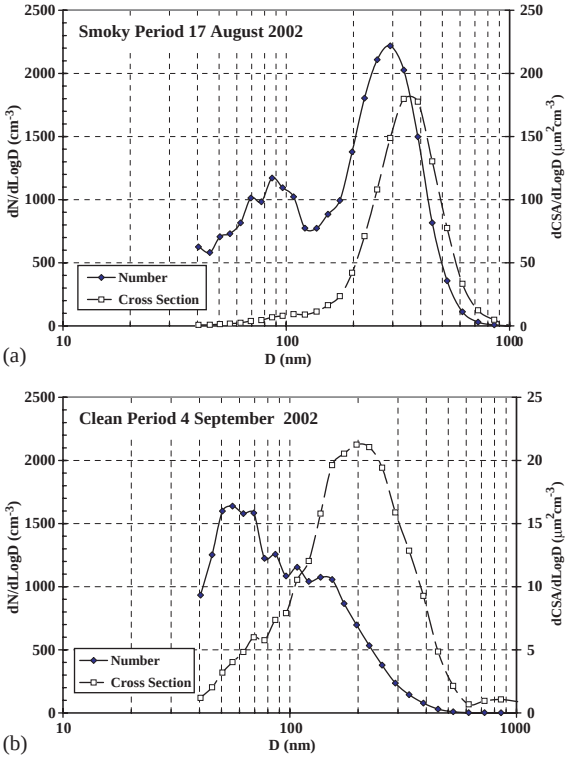


Fig. 6. Snapshot of "dry" number and cross-sectional area distributions during YACS as a function of particle diameter during (a) a smoky period (17 August 2002 DOY 229 1200–1400 PST) and (b) a relatively clean period (4 September 2002 DOY 247 1200-1400 PST). Number distributions are on the same scale but the cross-sectional area distribution scale is a factor of 10 higher during the smoky period in (a).

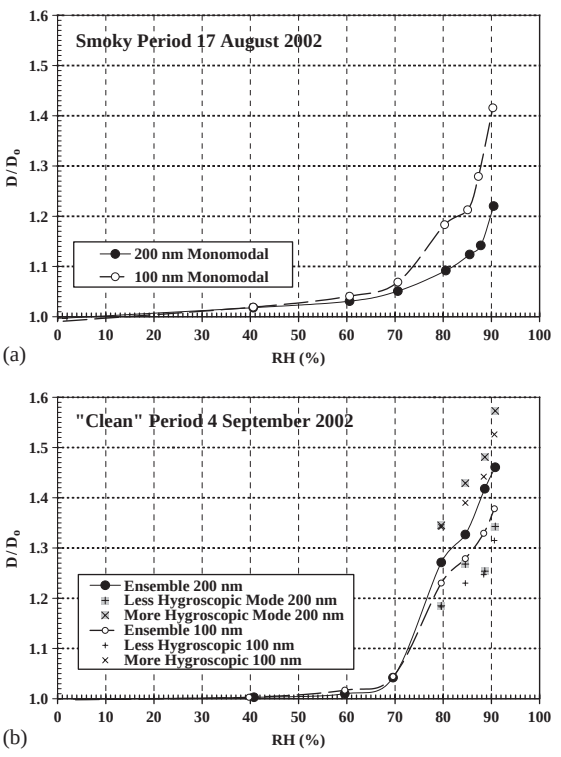


Fig. 7. Growth curves $D/D_o$ (RH) for 100 and 200 nm particles during YACS during (a) the period of strongest smoke impact 17 August 2002 (DOY 229) and (b) during a relatively clean period 4 September 2002 (DOY 247). Ensemble $D/D_o$ shown for 4 September is calculated as described in the methods by a cubic weighting of $D/D_o$ of individual modes that emerged for $\mathrm{RH}>80\%$.

the case of Fig. 7b. Growth curves during the "clean" period on 4 September showed stronger hygroscopicity for both sizes. In particular, 200 nm particles showed a sharp contrast between the two periods with $D(\mathrm{RH}=90\%)/D_o$ increasing from 1.2 (smoky period) to 1.5 ("clean" period).

Time series comparisons of ensemble $D(\mathrm{RH}=80\%)/D_o$ and chemical composition show a link between POM contribution and decreasing hygroscopicity (Fig. 5). A comparison of ensemble $D(\mathrm{RH}=80\%)/D_o$ vs. the mass ratio of POM to total inorganics (primarily $SO_4^{2-}$, $NH_4^+$, and $NO_3^-$) shows decreasing hygroscopicity with increasing POM fraction (Fig. 8). As the POM/ionic mass ratio exceeded 10, $D(\mathrm{RH}=80\%)/D_o$ approached 1.1. It should be noted that POM was a large fraction for most periods of HTDMA measurements. Only on DOY 247 (4 September 2002) was the ionic fraction greater than the POM fraction and consequently this day featured the largest $D/D_o$ measured during YACS (Fig. 5). Concurrent RH-controlled light scattering measurements likewise showed lower hygroscopic growth during POM-dominated periods (Malm et al., 2005).

A number of markers can be examined in relation to the hygroscopicity to explore the influence of biomass smoke. The difference in UV (350 nm) and near IR (880 nm) light absorption as measured with a multi-wavelength aethalometer (UV-IR, expressed in terms of the BC measurement unit of $\mu g\,m^{-3}$) is a qualitative indicator for biomass smoke. This is thought to be due to the enhanced UV absorption associated with POM components that are found in woodsmoke such as aromatic compounds [www.mageesci.com]. Biomass burning also releases a large amount of potassium rich submicrometer particles and thus the presence of non-seasalt soluble $K^+$ is also a smoke marker (Ma et al., 2003). From these markers, the large peak in POM during mid-August also featured a strong contribution from biomass smoke (Fig. 5), which from transport evidence was associated with massive regional wildfires (Malm et al., 2005; McMeeking et al., 2005).

Comparison of UV–IR averaged over the periods of $D/D_o$ measurements shows a relationship similar to the POM/ionic mass ratio (Fig. 8c, d). A higher POM fraction and periods of smoke influence (often coinciding during YACS) are both associated with decreasing hygroscopicity, particularly for 200 nm particles (Fig. 8). Ensemble $D(\mathrm{RH}=80\%)/D_o$ gives linear correlations with POM, POM/ions, aethalometer UV–IR, and soluble $K^+$ of $-0.74<R<-0.59$ for 200 nm and $-0.49<R<-0.25$ for 100 nm particles. Stronger relationships for 200 nm and a dominant less hygroscopic mode are likely related to a greater POM fraction in this size range (Fig. 8, Table 1). Typically, the dry size distribution showed dominance of particles with $D_p\sim$200–400 nm during smoke impacted periods (Fig. 6).

These findings are consistent with previous studies of water uptake of carbon-dominated aerosol. A study of ambient aerosol water uptake in the southeastern US inferred POM water uptake beginning at lower RH than ammoniated salts, though less strong hygroscopicity at RH > 80% (Dick et al., 2000). The study by Dick et al. (2000) observed $D(\mathrm{RH}=80\%)/D_o$ of 1.25–1.45 for ambient aerosols and derived water uptake estimates by the POM fraction equivalent to growth factors of $D(\mathrm{RH}=80\%)/D_o=1.15$ to 1.25. Similarly, ambient biogenic aerosols dominated by POM in Brazil had monomodal profiles and $D(\mathrm{RH}=90\%)/D_o$ of 1.16–1.32 while aerosols in forested Canadian sites near Vancouver showed both monomodal and bimodal hygroscopic growth profiles with $D(\mathrm{RH}=80\%)/D_o$ of 1.07–1.29 (Zhou et al., 2002; Aklilu and Mozurkewich, 2004). However, the POM composition may have been considerably different from this study as the previous studies featured a strong biogenic component not associated with smoke. For context, ambient marine boundary layer aerosols show strong hygroscopicity with typical $D(\mathrm{RH}=90\%)/D_o$ of 2–2.3 for sea salt particles and 1.6-1.8 for non-sea-salt $SO_4^{2-}$ (Berg et al., 1998). Measurements in urban areas typically show a nearly hygrophobic mode (soot) and a strongly hygroscopic mode (McMurry and Stoltzenburg, 1989; Cocker et al., 2001). Continental polluted aerosols have a typical $D(\mathrm{RH}=90\%)/D_o$ of 1–1.3 and 1.4–1.8 for the less and more hygroscopic modes (Swietlicki et al., 2000).

## 4. Summary and conclusions

Ambient aerosol composition during the Yosemite Aerosol Characterization Study in 2002 was dominated by POM (~70% of identified species). Chemical markers and transport patterns both suggested strong contributions to POM from pyrogenic and biogenic sources and little anthropogenic influence. Biomass smoke greatly affected aerosol physiochemical properties including water uptake during this study.

Measurements of particle diameter growth factors were performed with a humidified tandem differential mobility analyzer. Measurable water uptake began at intermediate RH (40–70%) with average $D(\mathrm{RH}=40\%, 60\%\text{ and }70\%)/D_o=1.01, 1.03$, and 1.06, respectively, for 200 nm particles. Beyond RH = 80%, the particles continued to take up water though relatively weakly with ensemble $D(\mathrm{RH}=80\%\text{ and }90\%)/D_o$ of $1.15\pm0.05$ and $1.31\pm0.06$, respectively, for 200 nm particles. Slightly larger $D/D_o$ were observed for 100 nm particles. Observed hygroscopic growth for the Yosemite POM-dominated aerosol was much lower than that for salts such as $(NH_4)_2SO_4$ and NaCl that typically comprise ambient aerosols in polluted and

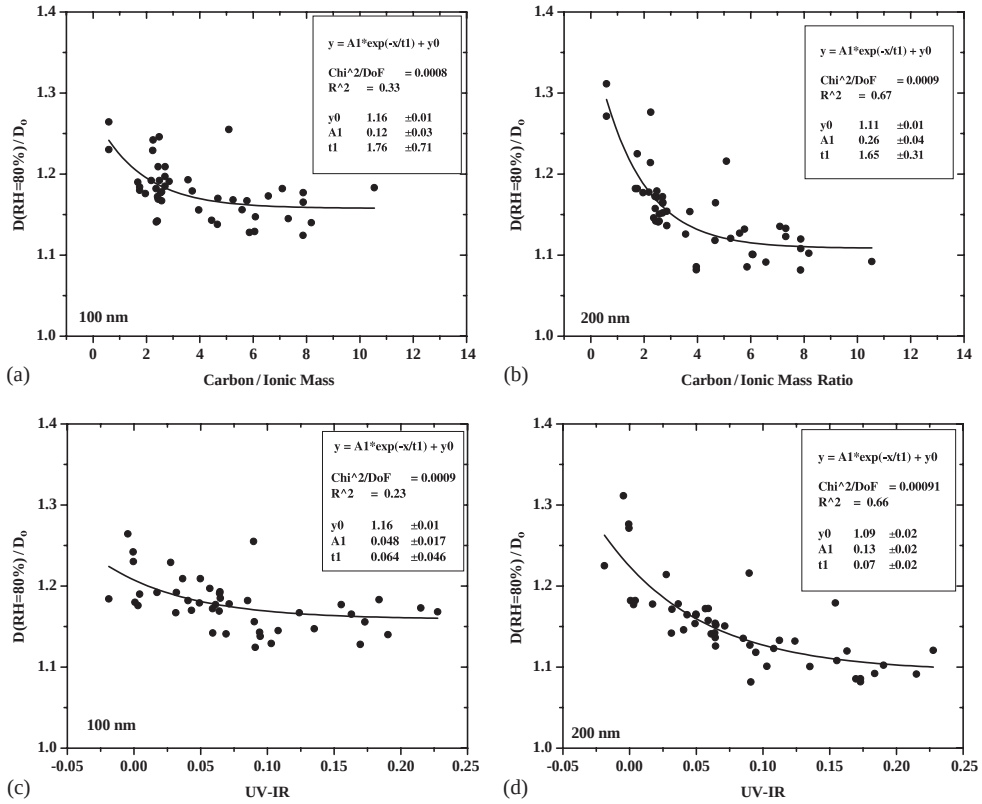


Fig. 8. Diameter growth factors ($D/D_o$ (RH = 80%)) for (a) 100 nm and (b) 200 nm particles vs. the 24 h average ratio of POM (from 24 h IMPROVE samples) to ionic mass concentration (from 24 h URG filter measurements) for $PM_{2.5}$ and vs. the difference in aethalometer 350 nm and 880 nm absorption (UV–IR) for (c) 100 nm and (d) 200 nm particles.

marine environments. $D/D_o$ at the average ambient RH of 33% was estimated to be below the detection limit (1.02) for the sizes considered here, suggesting a very small contribution by aerosol phase water to light extinction for this site and conditions.

Both monomodal and bimodal growth profiles were observed with bimodal dominating the 200 nm particles (68%). Separation into more and less hygroscopic modes occurred near RH = 80%. $D(\mathrm{RH} = 80\%)/D_o$ were $1.29 \pm 0.08$ and $1.11 \pm 0.04$ for more and less hygroscopic modes for 200 nm particles. Water uptake by 100 and 200 nm particles was overall very similar, though differences in the fraction of particles in less and more hygroscopic modes lead to a lower ensemble $D/D_o$ for 200 nm. Trimodal profiles with modes nearly as hygroscopic as pure $(NH_4)_2SO_4$, nearly hygrophobic, and similar to the experiment average hygroscopicity were observed twice during changing aerosol composition.

A clear relationship between increasing POM fraction and decreasing hygroscopicity was observed, particularly for 200 nm particles with $D(\mathrm{RH} = 80\%)/D_o = 1.1$ for ratios of POM/ionic mass exceeding 10. Smoke markers ($K^+$ and UV light absorption) showed similar inverse relationships, though less strong for 100 nm particles. The fraction of fine aerosol mass attributable to POM, independent of source, was the most important factor in reducing the hygroscopic growth. The results contribute to addressing important gaps in the knowledge of aerosol hygroscopic properties. This information is sparse in western US national parks that are often dominated by POM and strongly smoke impacted. Taken as a whole, the results suggest that aerosol phase water is a much smaller contributor to atmospheric extinction in POM dominated, smoke-impacted and low humidity environments, as compared to urban-industrial or marine environments. Such results have important ramifications to visibility impacts in national parks and radiative forcing of climate.

## Acknowledgments

The National Park Service supported this research (contract ♯CA2380-99001 TO0356). The authors gratefully acknowledge Air Resource Specialists, Inc., Russell Galipeau, Katy Warner, Jingchuan Zhou,

Mark Stolzenburg, Charles McDade, Lowell Ashbaugh, Thomas Cahill, Rodney Weber, Doug Orsini, Don Collins, and Andy Simpson for their assistance. We also thank two anonymous reviewers for constructive input that greatly improved this manuscript.

## References

Aklilu, Y.-A., Mozurkewich, M., 2004. Determination of external and internal mixing of organic and inorganic aerosol components from hygroscopic properties of submicrometer particles during a field study in the lower Fraser Valley. Aerosol Science and Technology 38, 140–154.

Ansari, A.S., Pandis, S.N., 2000. Water absorption by secondary organic aerosol and its effect an inorganic aerosol behavior. Environment Science and Technology 34 (1), 71–77.

Berg, O.H., Swietlicki, E., Krejci, R., 1998. Hygroscopic growth of aerosol particles in the marine boundary layer over the Pacific and Southern Oceans during the First Aerosol Characterization Experiment (ACE 1). Journal of Geophysical Research 103 (D13), 16,535–16,545.

Brechtel, F.J., Kreidenweis, S.M., 2000. Predicting particle critical supersaturation from hygroscopic growth measurement in the humidified TDMA: Part II: laboratory and ambient studies. Journal of Atmospheric Science 57, 1872–1887.

Brooks, S.D., DeMott, P.J., Kreidenweis, S.M., 2004. Water uptake by particles containing humic materials and mixtures of humic materials with ammonium sulfate. Atmospheric Environment, in press.

Carrico, C.M., Kus, P., Rood, M.J., Quinn, P.K., Bates, T., 2003. Mixtures of pollution, dust, and seasalt aerosol during ACE-Asia: light scattering properties as a function of relative humidity. Journal of Geophysical Research 108 (D23), 8650.

Cocker, D.R., Whitlock, N.E., Flagan, R.C., Seinfeld, J.H., 2001. Hygroscopic properties of Pasadena, California aerosol. Aerosol Science and Technology 35 (2), 637–647.

Dick, W.D., Saxena, P., McMurry, P.H., 2000. Estimation of water uptake by organic compounds in submicron aerosols measured during the southeastern aerosol and visibility study. Journal of Geophysical Research 105 (D1), 1471–1479.

Hand, J.L., Malm, W.C., Day, D., Lee, T., Carrico, J., Carrillo, J., Collett Jr., Laskin, A., Wang, C., Cowin, J.P., Iedema, M.J., 2005. Optical, physical and chemical properties of tar balls observed during the Yosemite Aerosol Characterization Study. Journal of Geophysical Research, submitted.

Hansson, H.-C., Rood, M.J., Koloutsou-Vakakis, S., Hämeri, K., Orsini, D., Wiedensohler, A., 1998. NaCl aerosol particle hygroscopicity dependence on mixing with organic compounds. Journal of Atmospheric Environment 31, 321–346.

Hobbs, P.V., Reid, J.S., Kotchenruther, R.A., Ferek, R.J., Weiss, R., 1997. Direct radiative forcing by smoke from biomass burning. Science 275, 1776–1778.

Iacobellis, S.F., Frouin, R., Somerville, R.C.J., 1999. Direct climate forcing by biomass-burning aerosols: impact of correlations between controlling variables. Journal of Geophysical Research 104 (D10), 12031–12045.

Kotchenruther, R.A., Hobbs, P.V., 1998. Humidification factors of aerosols from biomass burning in Brazil. Journal of Geophysical Research 103 (D24), 32,081–32,089.

Kreidenweis, S.M., Remer, L.A., Bruintjes, R., Dubovik, O., 2001. Smoke aerosol from biomass burning in Mexico: hygroscopic smoke optical model. Journal of Geophysical Research 106 (D5), 4831–4844.

Ma, Y., Weber, R.J., Lee, Y.-N., Orsini, D.A., Maxwell-Meier, K., Thornton, D.C., Bandy, A.R., Clarke, A.D., Blake, D.R., Sachse, G.W., Fuelberg, H.E., Kiley, C.M., Woo, J.-H., Streets, D.G., Carmichael, G.R., 2003. Characteristics and influence of biosmoke on the fine-particle ionic composition measured in Asian outflow during the Transport and Chemical Evolution over the Pacific (TRACE-P) experiment. Journal of Geophysical Research 108 (D21), 8816.

Malm, W.C., Kreidenweis, S.M., 1997. The effects of model of aerosol hygroscopicity on the apportionment of extinction. Atmospheric Environment 31 (13), 1965–1976.

Malm, W.C., Day, D.E., 2001. Estimates of aerosol species scattering characteristics as a function of relative humidity. Atmospheric Environment 35, 2845–2860.

Malm, W.C., Day, D.E., Kreidenweis, S.M., Collett, J.L., Lee, T., 2003. Humidity-dependent optical properties of fine particles during the big bend regional aerosol and visibility observational study. Journal of Geophysical Research 108 (D9), 4279.

Malm, W.C., Schichtel, B.A., Pitchford, M.L., Ashbaugh, L.L., Eldred, R.A., 2004. Spatial and monthly trends in speciated fine particle concentration in the United States. Journal of Geophysical Research 109.

Malm, W.C., Day, D.E., Carrico, C., Kreidenweis, S.M., Collett Jr., J.L., McMeeking, G., Lee, T., Carillo, J., 2005. Inter-comparison and closure calculations using measurements of aerosol species and optical properties during the Yosemite Aerosol Characterization Study. Journal of Geophysical Research, accepted.

Markowicz, K.M., Flatau, P.J., Quinn, P.K., Carrico, C.M., Flatau, M.K., Vogelmann, A.M., Bates, D., Liu, M., Rood, M.J., 2003. Influence of relative humidity on aerosol radiative forcing: an ACE-Asia experiment perspective. Journal of Geophysical Research 108 (D23), 8662.

McKenzie, L.M., Hao, W.M., Richards, G.N., Ward, D.E., 1995. Measurement and modeling of air toxins from smoldering combustion of biomass. Environmental Science and Technology 29 (8), 2047–2054.

McMeeking, G.R., Kreidenweis, S.M., Carrico, C., Lee, T., Collett, J.L., Malm, W.C., 2005. Observations of smoke influenced aerosol during the Yosemite Aerosol Characterization Study Part I: size distributions and chemical composition. Journal of Geophysical Research, submitted.

McMurry, P.H., Stoltzenburg, M.R., 1989. On the sensitivity of particle size to relative humidity for Los Angeles aerosols. Atmospheric Environment 23 (2), 497–507.

Park, R.J., Jacob, D.J., Chin, M., Martin, R.V., 2003. Sources of carbonaceous aerosols over the United States and implications for natural visibility. Journal of Geophysical Research 108 (D12), 4355.

Penner, J.E., Dickinson, R.E., O'Neill, C.A., 1992. Effects of aerosols from biomass burning on the global radiation budget. Science 256, 1432–1433.

Pilinis, C., Pandis, S.N., Seinfeld, J.H., 1995. Sensitivity of direct climate forcing by atmospheric aerosols to aerosol size and composition. Journal of Geophysical Research 100, 18,739–18,754.

Prenni, A.J., Demott, P.J., Kreidenweis, S.M., 2003. Water uptake of internally mixed particles containing ammonium sulfate and dicarboxylic acids. Atmospheric Environment 37, 4243–4251.

Rader, K.J., McMurry, P.H., 1986. Application of the tandem differential mobility analyzer to studies of droplet growth and evaporation. Journal of Aerosol Science 17, 771–787.

Riebau, A.R., Fox, D., 2001. The new smoke management. International Journal of Wildland Fire 2001 (10), 415–427.

Saxena, P., Hildemann, L.M., McMurry, P.H., Seinfeld, J.H., 1995. Organics alter hygroscopic behavior of atmospheric particles. Journal of Geophysical Research 100 (D9), 18755–18770.

Saxena, P., Hildemann, L.M., 1996. Water-soluble organics in atmospheric particles: a critical review of the literature and application of thermodynamics to identify candidate compounds. Journal of Atmospheric Chemistry 24, 57–109.

Stolzenburg, M.R., McMurry, P.H., 1988. TDMAFIT User's Manual. PTL Publications No.653, Particle Technology Laboratory, Department of Mechanical Engineering, University of Minnesota, Minneapolis, MN, USA.

Sullivan, T.J., Peterson, D.L., Blanchard, C.L., Tanenbaum, S.J., 2001. Assessment of Air Quality and Air pollutant Impacts in Class I National Parks of California, US, Department of Interior-National Park Service, NPS D-1454, April 2001.

Swietlicki, E., Zhou, J., Covert, D.S., Hämeri, K., Busch, B., Väkeva, M., Dusek, U., Berg, O., Wiedensohler, A., Aalto, P., Mäkelä, J., Martinsson, B., Papaspiropoulos, G., Mentes, B., Frank, G., Stratmann, F., 2000. Hygroscopic properties of aerosol particles in the northeastern Atlantic during ACE-2. Tellus 52B, 201–227.

Tang, I.N., Munkelwitz, H.R., 1993. Composition and temperature dependence of the deliquescence properties of hygroscopic aerosols. Atmospheric Environment 27A (4), 467–473.

Tang, I.N., Munkelwitz, H.R., 1994. Water activities, densities, and refractive indices of aqueous sulfates and sodium nitrate droplets of atmospheric importance. Journal of Geophysical Research 99, 18,801–18,808.

US Environmental Protection Agency (US EPA), 1999. Federal Register, 40 CFR Part 51, vol 64, No. 126, Docket No. A-95-38, 35,714–35,774.

Wotawa, G., Trainer, M., 2000. The influence of Canadian forest fires on pollutant concentrations in the United States. Science 288, 324–328.

Zhang, X.Q., McMurry, P.H., Hering, S.V., Casuccio, G.S., 1993. Mixing characteristics and water content of submicron aerosols measured in Los Angeles and at the Grand Canyon. Atmospheric Environment 27A, 1593–1607.

Zhou, J., Swietlicki, E., Hansson, H.C., Artaxo, P., 2002. Submicrometer aerosol particle size distribution and hygroscopic growth measured in the Amazon rain forest during the wet season. Journal of Geophysical Research 107 (D20), 8055.